Inhibition of the p-SPAK/p-NKCC1 signaling pathway protects the blood-brain barrier and reduces neuronal apoptosis in a rat model of surgical brain injury

YATING GONG[1*], MUYAO WU[1*], FAN GAO[1], MENGYING SHI[2], HAIPING GU[3], RONG GAO[4], BAO-QI DANG[1] and GANG CHEN[5]

Departments of [1]Rehabilitation, [2]Anesthesiology, [3]Neurology and [4]Neurosurgery, Zhangjiagang Traditional Chinese Medicine Hospital Affiliated to Nanjing University of Chinese Medicine, Suzhou, Jiangsu 215600; [5]Brain and Nerve Research Laboratory, Department of Neurosurgery, The First Affiliated Hospital of Soochow University, Suzhou, Jiangsu 215006, P.R. China

Received November 19, 2020; Accepted May 7, 2021

DOI: 10.3892/mmr.2021.12356

Abstract. Surgical brain injury (SBI) can disrupt the function of the blood-brain barrier (BBB), leading to brain edema and neurological dysfunction. Thus, protecting the BBB and mitigating cerebral edema are key factors in improving the neurological function and prognosis of patients with SBI. The inhibition of WNK lysine deficient protein kinase/STE20/SPS1-related proline/alanine-rich kinase (SPAK) signaling ameliorates cerebral edema, and this signaling pathway regulates the phosphorylation of the downstream Na^+-K^+-Cl^- cotransporter 1 (NKCC1). Therefore, the purpose of the present study was to investigate the role of SPAK in SBI-induced cerebral edema and to determine whether the SPAK/NKCC1 signaling pathway was involved in SBI via regulating phosphorylation. An SBI model was established in male Sprague-Dawley rats, and the effects of SPAK on the regulation of the NKCC1 signaling pathway on BBB permeability and nerve cell apoptosis by western blotting analysis, immunofluorescence staining, TUNEL staining, Fluoro-Jade C staining, and brain edema and nervous system scores. The results demonstrated that, compared with those in the sham group, phosphorylated (p)-SPAK and p-NKCC1 protein expression levels were significantly increased in the SBI model group. After inhibiting p-SPAK, the expression level of p-NKCC1, neuronal apoptosis and BBB permeability were significantly reduced in SBI model rats. Taken together, these findings suggested that SBI-induced increases in p-SPAK and p-NKCC1 expression exacerbated post-traumatic neural and BBB damage, which may be mediated via the ion-transport-induced regulation of cell edema.

Correspondence to: Dr Rong Gao, Department of Neurosurgery, Zhangjiagang Traditional Chinese Medicine Hospital Affiliated to Nanjing University of Chinese Medicine, 77 Changan Southern Road, Suzhou, Jiangsu 215600, P.R. China
E-mail: 714866001@qq.com

Dr Bao-Qi Dang, Department of Rehabilitation, Zhangjiagang Traditional Chinese Medicine Hospital Affiliated to Nanjing University of Chinese Medicine, 77 Changan Southern Road, Suzhou, Jiangsu 215600, P.R. China
E-mail: zhenjiangdbq@163.com

*Contributed equally

Key words: surgical brain injury, STE20/SPS1-related proline/alanine-rich kinase, Na^+-K^+-Cl^- cotransporter 1, blood-brain barrier, brain edema, neuroprotection

Introduction

Neurosurgery improves the survival rate and quality of life of patients. However, the invasive nature of neurosurgery can occasionally induce non-traumatic injury, namely, surgical brain injury (SBI) (1). Due to incision, electrocoagulation, bleeding and other invasive operations in the process of brain surgery, there will be some damage to the brain tissue surrounding the operation site, which may lead to peripheral tissue damage, edema, apoptosis and inflammation (2). Among these pathologies, cerebral edema leads to postoperative neurological dysfunction, which is one of the primary adverse reactions of SBI (3). Thus, the reduction of cerebral edema after SBI is beneficial for improving neural function, postoperative recovery and patient prognosis (4,5). The prevention and treatment of brain edema before brain surgery has become a possible therapeutic target for reducing SBI (6). However, the mechanism and preventative treatment of postoperative cerebral edema requires further investigation.

As the most common complication after SBI, brain edema is caused by the close connection of vascular endothelial cells and the destruction of astrocytes and other components of the blood-brain barrier (BBB), thereby damaging the BBB and exacerbating brain injury (7). Previous studies have shown that the WNK lysine deficient protein kinase 3 (WNK3)/STE20/SPS1-related proline/alanine-rich kinase (SPAK) signaling pathway serves an important role in the

process of brain edema (8-10). It has been revealed that inhibiting the expression levels of components of this signaling pathway can reduce BBB damage, as well as decrease the degree of brain edema and neurobehavioral dysfunction (11). SPAK is involved in brain edema via regulating the downstream Na^+-K^+-Cl^- cotransporter 1 (NKCC1) (12). NKCC1 regulates the entry of Na^+, K^+, Cl^- and water into cells, maintains concentrations of intracellular ions/water, ensures homeostasis of the intracellular environment, contributes to BBB-selective ion permeability and regulates cellular volume (13,14). SPAK is a key effector in regulating ion flow and balance (15). When SPAK interacts with downstream NKCC1, it serves a related role in regulating ion transport, increasing cellular volume and influencing cellular homeostasis (11,16). After brain injury, the expression levels of proteins in the WNK family are upregulated, and they associate with and activate SPAK via the phosphorylation of the T-loop at Thr233/Thr185 (17). Upon its activation through phosphorylation by upstream kinases, phosphorylated (p)-SPAK binds to specific peptides located in the cytosolic tail of NKCC1, whereby it phosphorylates NKCC1 and stimulates cotransport activity (18). Moreover, increased expression and activity of p-SPAK/p-NKCC1 increases the entry of extracellular ions and water into cells (19). This process induces the enlargement of neurons, glial cells and endothelial cells, destroys the cytoskeleton structure of cells, and leads to cell swelling and apoptosis, which can damage the BBB, resulting in brain edema and neurological dysfunction (11,20).

The SPAK/NKCC1 signaling pathway has been reported to serve an important role in the pathophysiology of brain diseases, such as stroke (21), traumatic brain injury (22) and subarachnoid hemorrhage (23). However, the role and mechanism of this signaling pathway in SBI are yet to be fully elucidated. The aim of the present study was to investigate the influence of the SPAK/NKCC1 signaling pathway on the BBB and neural function in a rat model of SBI. Closantel, an anti-parasitic agent that is widely used in livestock (24), was used to inhibit SPAK. Closantel inhibits SPAK by binding to a C-terminal domain at a highly conserved allosteric site (25). Furthermore, closantel has been shown to successfully inhibit SPAK, thereby reducing p-NKCC1 expression in the aorta (26).

Materials and methods

Experimental design and groupings. The present study consisted of two separate experiments, the designs and groupings of which are depicted in Fig. 1A-C.

Experiment 1: There was no significant difference in weight, food intake or exercise among the different groups. In total there were 38 rats in experiment 1, 36 of which survived surgeries and were randomly divided into six groups (n=6 per group) consisting of a sham-operation group and five experimental groups (6, 12, 24, 48 and 72 h after SBI operations). The experimental rats were all sacrificed at their designated time points after SBI, at which time brain tissue was harvested from around the damaged area. Western blot (WB) analysis was performed on part of this harvested brain tissue, whereas the rest of the brain tissue was used for double immunofluorescence (IF) analyses.

Experiment 2: A total of 51 rats were included in experiment 2, 48 rats survived and were randomly divided into the following four groups (n=12 per group): i) Sham; ii) SBI; iii) SBI + vehicle; and iv) SBI + closantel. According to the results of experiment 1, rats (n=6 per group) were sacrificed at 48 h after SBI in experiment 2, and brain tissues surrounding the damaged area were used for WB analysis, IF, TUNEL and Fluoro-Jade C (FJC) staining assays. Brain tissue from the remaining six rats in each group was used to measure brain edema. Neurological examinations were performed in all groups prior to sacrifice.

Experimental animals. All experiments received approval from the Institute of Animal Care Committee of Zhangjiagang Traditional Chinese Medicine Hospital (approval no. 2020-10-1; Suzhou, China), and were performed in accordance with the Chinese Association for Laboratory Animal Sciences (27). A total of 89 male Sprague-Dawley rats (age, 8 weeks; weight, 320-350 g) were purchased from the Zhaoyan (Suzhou) New Drug Research Center Co., Ltd. All rats were raised at a temperature of ~26˚C, with a humidity of ~50%, and light/dark periods identical to outdoor conditions. Food and water were provided *ad libitum*.

Establishment of SBI model in rats. A rat model of SBI was established as previously reported (28). Sprague-Dawley rats were anesthetized via an intraperitoneal injection of sodium pentobarbital (10 mg/ml; 40 mg/kg). The rats were then prone and fixed in a stereotaxic apparatus (Yuyan Instruments). An incision was made along the midline of the skin above the brain to expose the skull in order to identify bregma. Then, a 5x5 mm craniotomy was performed on the right frontal skull by removing a bone flap using a bone drill from the right skull bone 2-mm along the sagittal suture and 1-mm along coronal suture. A durotomy was performed and 2x3 mm brain tissue was excised via sharp dissection. An electrocautery unit was used to stop bleeding, after which the area was rinsed with normal saline. In the sham rats, the same surgical method was used; a craniotomy was performed to remove the bone flap, but part of the right frontal lobe was not removed. Important parameters of interest were monitored during and after surgery, including heart rate, body temperature and body weight. According to the experimental requirements, the rats were sacrificed via an intraperitoneal injection of sodium pentobarbital (20 mg/ml; 150 mg/kg) at different time points (Fig. 1).

Drug injections. The experimental 2 rats were divided into the following four groups: i) Sham; ii) SBI; iii) SBI + vehicle; and iv) SBI + closantel. The SBI + closantel group was intraperitoneally injected with 20 mg/kg closantel (Abcam) at 30 min before SBI, as previously described (26). The weight-matched SBI + vehicle group was intraperitoneally injected with an equal volume of 10% DMSO.

Neurological scoring. The neurological function of each rat was evaluated according to the scale before sacrifice. Neurological scoring was conducted as previously reported (29) and consisted of the following seven components: i) Symmetry of limb movement; ii) forelimb-stretching exercises; iii) lateral turning; iv) climbing; v) body movements; vi) proprioception;

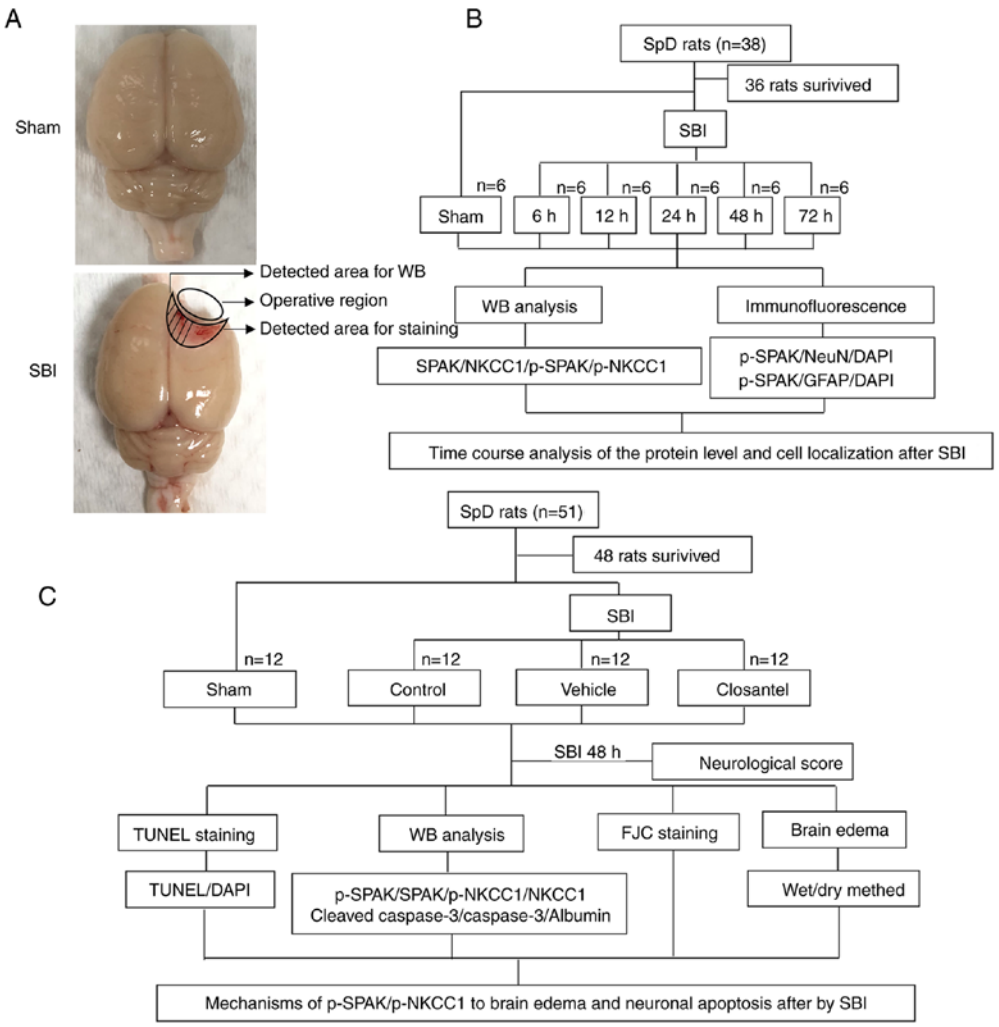

Figure 1. SBI model and experimental design. (A) Brain tissue from the same location in the sham group as that injured in the SBI group was obtained for testing; some tissues were used for WB analysis, whereas the remaining tissues were used for staining. (B) Expression levels of SPAK, p-SPAK, NKCC1 and p-NKCC1, as well as cellular localization of p-SPAK and p-NKCC1 were assessed after SBI to determine suitable time points for subsequent experiments. (C) The role and mechanism of the p-SPAK/p-NKCC1 signaling pathway in early brain injury after SBI was investigated. SBI, surgical brain injury; p, phosphorylated; FJC, Fluoro-Jade C; SpD, Sprague-Dawley; SPAK, STE20/SPS1-related proline/alanine-rich kinase; NKCC1, Na^+-K^+-Cl^- cotransporter 1; WB, western blot; NeuN, neuronal nuclei; GFAP, glial fibrillary acidic protein.

and vii) responses to vibrissae touch. Scores on each subtest ranged from 0-3, with a combined maximum score of 21. Higher scores were indicative of reduced neurological damage (i.e., 21, no neurological deficits).

Tissue collection and sectioning. To isolate proteins, rats were perfused with 200 ml 0.9% normal saline (at 4˚C) through the heart and cortical samples <3 mm from the contusion edge were collected on ice (Fig. 1A). Some brain tissue samples (n=6 rats per group) were immediately frozen and stored at -80˚C until subsequent WB analysis. To obtain brain sections, brains were harvested, immersed in 4% paraformaldehyde at 4˚C for >48 h and then embedded in paraffin. Paraffin-embedded brain sections were sectioned using a paraffin slicing machine to a thickness of 5-μm each. All procedures for tissue removal and selection were performed by two pathologists who were blinded to the experimental conditions.

WB analysis. WB analysis was performed as described previously (30). The extracted brain tissue was homogenized in tissue protein-extraction reagent with a protease inhibitor cocktail (CWBio) and incubated on ice for 20 min. Subsequently, the homogenized brain tissue was centrifuged at 12,000 x g at 4˚C for 20 min. The supernatant was then collected and protein concentrations were determined using the Pierce TM BCA protein-detection kit (Thermo Fisher Scientific, Inc.). Then, 8, 10 and 12% gels (Beyotime Institute of Biotechnology) were used according to the different molecular weights. The extracted proteins were loaded onto SDS-polyacrylamide gels at 3 mg per lane. These electrophoresed proteins were then transferred to a PVDF membrane (EMD Millipore). WB quick seal liquid (Beyotime Institute of Biotechnology) was used to block the PVDF membrane for 30 min at room temperature. Samples were then incubated with primary antibodies at 4˚C overnight, including: Rabbit anti-SPAK (1:1,000; cat. no. 2281; Cell Signaling Technology, Inc.), mouse anti-NKCC1 (1:500; cat. no. sc-514774; Santa Cruz Biotechnology, Inc.), sheep anti-p-SPAK (1:400; cat. no. S668B; MRC Protein Phosphorylation and Ubiquitylation Unit), sheep anti-p-NKCC1 (1:400; cat. no. S763B; MRC Protein

Phosphorylation and Ubiquitylation Unit), rabbit anti-GAPDH (1:5,000; cat. no. G9545; Sigma-Aldrich; Merck KGaA), rabbit anti-Albumin (1:1,000; cat. no. ab207327; Abcam), rabbit anti-cleaved-Caspase-3 (1:1,000; cat. no. 9664; Cell Signaling Technology, Inc.) and rabbit anti-Caspase-3 (1:1,000; cat. no. ab184787; Abcam). After washing three times with PBS, samples were incubated with secondary antibodies for 2 h at 4˚C, including goat anti-mouse IgG-HRP (1:5,000; cat. no. 91196; Cell Signaling Technology, Inc.), goat anti-rabbit IgG-HRP (1:5,000; cat. no. 31466; Invitrogen; Thermo Fisher Scientific, Inc.) and rabbit anti-sheep IgG-HRP (1:2,000; cat. no. 81-8620; Thermo Fisher Scientific, Inc.). Immunoblots were probed with the Immobilon Western Chemiluminescent HRP substrate (EMD Millipore) and visualized using an imaging system (Teledyne Photometrics). All data were analyzed using ImageJ software (v 1.8.0; National Institutes of Health). GAPDH was used as the loading control.

IF staining. Double-IF staining was conducted as previously described (31). The paraffin-embedded sections were heated at 70˚C for 1 h in an oven, soaked in xylene, rehydrated in anhydrous ethanol, 95, 85 and 70% ethanol, and then repaired with sodium citrate. Following three washes with PBS, the membranes were permeabilized using immunostaining permeable solution (Beyotime Institute of Biotechnology). The brain sections were covered for ≥30 min with immunostaining-blocking solution (Beyotime Institute of Biotechnology) at room temperature, after which samples were incubated with primary antibodies at 4˚C overnight. After three washes in PBS, samples were incubated with secondary antibodies at room temperature for 1 h. Finally, the samples were counterstained with DAPI (Shanghai Yeasen Biotechnology Co., Ltd.) at room temperature for 10 min and observed under a fluorescent microscope (Olympus Corporation). The following antibodies were used: Sheep anti-p-SPAK (1:100; cat. no. S668B; MRC Protein Phosphorylation and Ubiquitylation Unit), mouse anti-glial fibrillary acidic protein (GFAP; 1:400; cat. no. 14-9892-95; Invitrogen; Thermo Fisher Scientific, Inc.), mouse anti-neuronal nuclei (NeuN; 1:1,000; cat. no. ab104224; Abcam), donkey anti-Sheep IgG, Alexa Fluor 488 (1:800; cat. no. A-11015; Invitrogen; Thermo Fisher Scientific, Inc.) and donkey anti-mouse IgG, Alexa Fluor 555 (1:800; cat. no. A32787TR; Invitrogen; Thermo Fisher Scientific, Inc.).

TUNEL staining. Apoptosis was detected in the paraffin-embedded sections using a TUNEL Apoptosis Detection Kit (Beyotime Institute of Biotechnology) according to the manufacturer's protocols. The paraffin-embedded section dewaxing steps were performed according to the aforementioned protocol described in the IF staining section. Sections were washed with distilled water for 2 min and then incubated in a protease-K working solution for 30 min at 37˚C. Thereafter, samples were washed three times in PBS (5 min each time). Brain sections were covered with TUNEL working solution and incubated in a damp box at 37˚C in the dark for 1 h. Samples were then washed three times in PBS (5 min each time). Finally, the mounting medium containing DAPI (Shanghai Yeasen Biotechnology Co., Ltd.) was applied at room temperature for 10 min and observed under a fluorescent microscope (Olympus Corporation). Each brain tissue was observed under a microscope in a random selection of six fields of vision around the damaged area.

FJC staining. FJC Ready-to-Dilute Staining Kit (Biosensis Pty, Ltd.) was used as per the manufacturer's instructions. Paraffin-embedded sections were incubated in an oven at 70˚C for 1 h. Then, samples were rehydrated in a descending alcohol series consisting of xylene, 100% ethanol and 70% ethanol. Subsequently, samples were washed twice with double-distilled H_2O for 1 min at room temperature before being cleaned with distilled water for 2 min at room temperature. Then, nine parts of distilled water were mixed with one part of solution B (potassium permanganate), which the slides were then incubated in for 10 min at room temperature. Subsequently, slides were rinsed for 2 min in distilled water. Then, nine parts of distilled water were mixed with one part of solution C, and samples were incubated in the dark for 10 min at room temperature. After washing three times with distilled water, samples were dried in an oven at 60˚C for ≥5 min. Then, samples were soaked in xylene for 5 min at room temperature. After drying, samples were sealed with neutral resin in liquid (Shanghai Yeasen Biotechnology Co., Ltd.) and observed under a fluorescent microscope.

Brain edema. Brain edema was assessed by determining the moisture content of the brain using the wet-dry method (32,33). After separation of rat brain tissues, the brains were divided into ipsilateral and contralateral hemispheres, and were quickly weighed to determine their wet weights. Then, the brain samples were dried in an oven at 100˚C for 24 h, and subsequently weighed to determine their dry weights. The percentage of brain water content (%) was calculated as follows: [(Wet weight-dry weight)/(wet weight)] x100%.

Statistical analysis. The experiments were repeated six times. All data are presented as the mean ± SD. GraphPad Prism 8.0 software (GraphPad Software, Inc.) was used for all statistical analyses. One-way ANOVA followed by Tukey's post hoc test was used for multiple comparisons to determine the differences among all groups. IF staining were analyzed using an unpaired Student's t-test. Neurological behavioral scores among different groups were analyzed using the Kruskal-Wallis test followed by Dunn's post hoc test. $P<0.05$ was considered to indicate a statistically significant difference.

Results

Post-SBI protein expression levels of SPAK, p-SPAK, NKCC1 and p-NKCC1 in the brain. The expression levels of SPAK, p-SPAK, NKCC1 and p-NKCC1 at 6, 12, 24, 48 and 72 h after SBI, as well as in sham rats, were assessed via WB analysis. Compared with those in the sham group, there was no significant change in SPAK or NKCC1 expression, whereas p-SPAK expression was significantly increased beginning at 6 h after SBI and reaching a peak at 48 h post-SBI (Fig. 2A and B). Additionally, compared with the sham group, p-NKCC1 expression was significantly increased beginning at 12 h after SBI and reaching a peak at 48 h post-SBI (Fig. 2C and D).

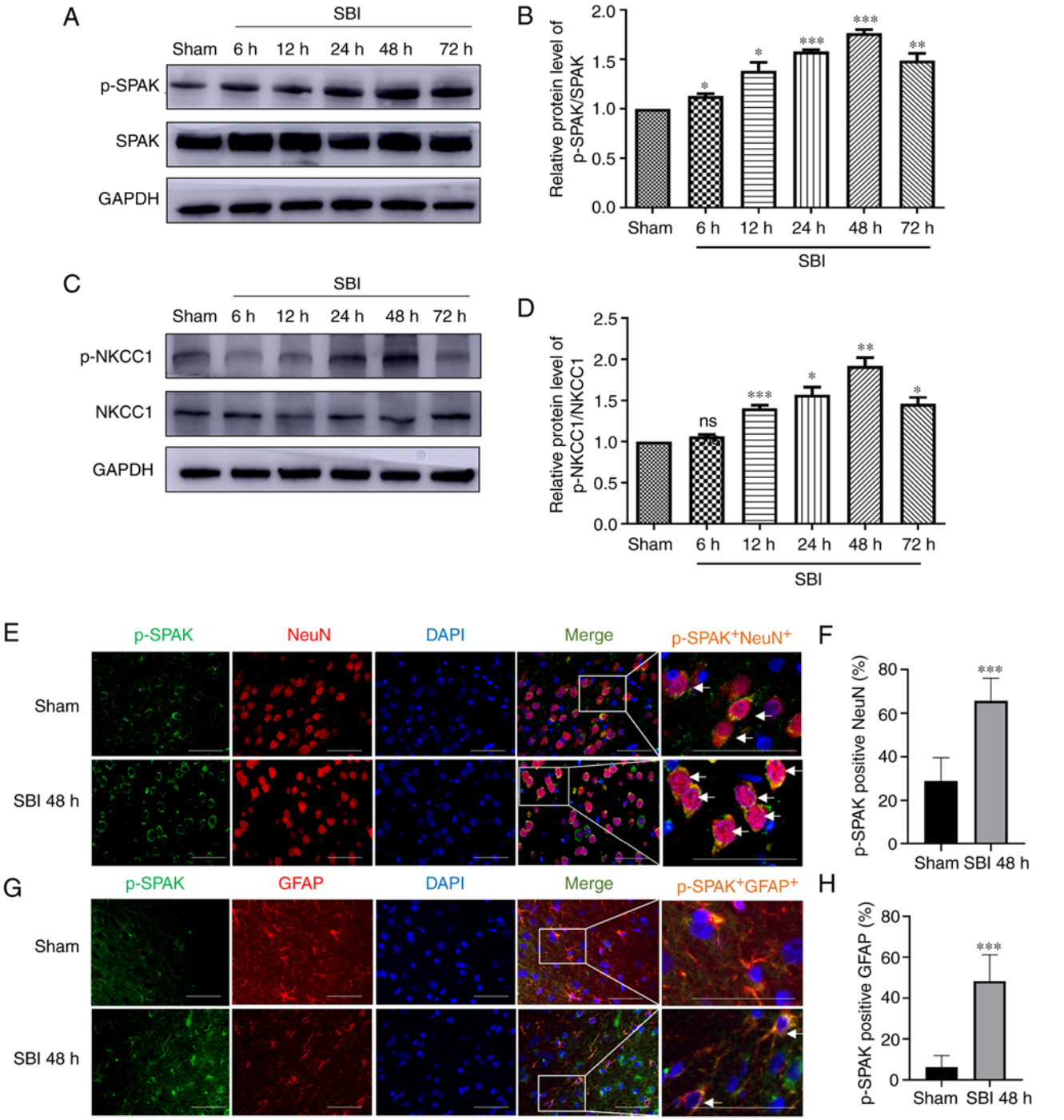

Figure 2. Protein expression levels of SPAK, p-SPAK, NKCC1 and p-NKCC1 in the lesion of the peripheral cortex after SBI injury. SPAK/p-SPAK protein expression levels at 6, 12, 24, 48 and 72 h in the SBI groups and in the sham group were (A) determined by WB analysis and (B) semi-quantified. p-NKCC1/NKCC1 protein expression levels at 6, 12, 24, 48 and 72 h in the SBI groups and in the sham group were (C) determined by WB analysis and (D) semi-quantified. The relative densities of each protein were standardized to those of the sham group. ImageJ software was used to semi-quantify the protein expression, and the mean value of the sham group was normalized to 1. Statistical analysis was performed using one-way ANOVA followed by Tukey's post hoc test. Double IF staining images of p-SPAK in the peripheral cortex of the damaged area. In the sham group and at 48 h after SBI, the expression profiles of green-labeled p-SPAK and red-labeled (E and F) NeuN/(G and H) GFAP were identified by performing double IF staining. The nuclei were labeled with DAPI (blue) fluorescence. Arrows indicate the co-localization of p-SPAK with NeuN/GFAP. Scale bar, 50 μm; The images for p-SPAK, NeuN/GFAP, DAPI and Merge are at x400 magnification. Statistical analyses were performed using an unpaired Student's t-test. Data are presented as the mean ± SD (n=6 per group). *P<0.05, **P<0.01 and ***P<0.001 vs. sham. SPAK, STE20/SPS1-related proline/alanine-rich kinase; NKCC1, Na^+-K^+-Cl^- cotransporter 1; NeuN, neuronal nuclei; GFAP, glial fibrillary acidic protein; SBI, surgical brain injury; p, phosphorylated; IF, immunofluorescence; ns, not significant; WB, western blot.

Post-SBI p-SPAK expression in peri-injury cortical cells. p-SPAK expression was assessed via IF staining with a NeuN marker and astrocytic (GFAP) marker. The expression level of p-SPAK in $NeuN^+$ cells is shown in Fig. 2E and F, and that in $GFAP^+$ cells is presented in Fig. 2G and H. The analyses revealed that the numbers of p-$SPAK^+$ neurons and astrocytes in the 48 h post-SBI group were significantly increased compared with those of the sham group.

Closantel decreases p-SPAK and p-NKCC1 expression after SBI. It was found that p-SPAK expression was significantly higher in the SBI and SBI + vehicle groups compared with that in the sham group (Fig. 3A and B). Moreover, after closantel intervention, p-SPAK expression was significantly decreased in the closantel group compared with that in the SBI + vehicle group, as demonstrated by WB analysis. Additionally, after closantel intervention, p-NKCC1 expression was significantly decreased compared with that in the SBI + vehicle group (Fig. 3C and D). The trend for cleaved-caspase-3 expression was similar to that of p-SPAK expression across these groups (Fig. 3E and F).

Closantel ameliorates the BBB and neurobehavioral scores in SBI model rats. Then, the integrity of the BBB was assessed by measuring albumin and brain wet-dry specific weight. Albumin expression was significantly higher in the SBI group and SBI + vehicle group compared with that in the sham group (Fig. 3G and H). After closantel intervention, albumin expression was significantly decreased in the closantel group compared with that in the SBI + vehicle group.

After SBI, brain edema in the damaged hemispheres was significantly reduced by closantel intervention (Fig. 3I). However, there was no significant change in brain water content in the contralateral hemispheres. These results confirmed that there was a significant impairment of the BBB after SBI, which was mitigated following closantel intervention. Compared with those of the sham group, the neurological scores of rats in the SBI group and SBI + vehicle group were significantly lower (Fig. 3J). Furthermore, compared with those of the SBI + vehicle group, the neurobehavioral scores of rats were significantly improved in the SBI + closantel group. These results indicated that the neurobehavioral scores were significantly improved after SBI + closantel intervention.

Effect of closantel intervention on neuronal degeneration and apoptosis after SBI. TUNEL staining was used to detect apoptotic cells in the brain tissue surrounding the injured area. The degree of neuronal apoptosis in the SBI and SBI + vehicle groups was significantly higher compared with that in the sham group (Fig. 4A and B). Additionally, the degree of apoptosis in the SBI + closantel group was significantly lower compared with that in the SBI + vehicle group. Neuronal degeneration was detected via FJC staining. The trend for FJC staining was similar to the TUNEL staining results across these groups (Fig. 4C and D). These results suggested that closantel intervention significantly improved neuronal degeneration and apoptosis in SBI model rats.

Discussion

The present study investigated the neuroprotective effect of inhibiting SPAK in the SBI rat model and evaluated its potential mechanism. The current results demonstrated that, compared with the sham group, the protein expression level of p-SPAK began to increase at 6 h after SBI and reached a peak by 48 h, after which it began to decline. Furthermore, inhibition of p-SPAK expression significantly reduced albumin expression, cell apoptosis, brain edema and neurological impairment in SBI model rats. After SBI, p-NKCC1 expression increased slightly later compared with that of p-SPAK. Furthermore, when p-SPAK expression was decreased, p-NKCC1 expression was also decreased. These results indicated that, in the current SBI rat model, NKCC1 may be located downstream of SPAK and may be regulated by SPAK. Moreover, inhibiting p-SPAK may reduce secondary brain injury caused by SBI.

Secondary brain edema is caused by the destruction of the original ion homeostasis, which leads to changes to brain tissue cell volume and homeostasis (34). Leakage of the BBB leads to albumin extravasation, which in turn increases inflammation and edema, thus exacerbating brain damage (35,36). Lu *et al* (37) reported that the mRNA and protein expression levels of NKCC1 were upregulated in the neurons of animals with traumatic brain injury, and the animals displayed severe brain edema and neuronal damage. NKCC1 belongs to the cation-Cl^- cotransporters and is an important determinant of ion homeostasis in the brain (38). In the central nervous system, intracellular Cl^- concentrations are determined by NKCC1, and the two chloride ion channels have been identified as novel targets for the treatment of cerebral edema (23,39). SPAK is the primary regulator of cation-chloride cotransporters and stimulates NKCC1 ion influx via phosphorylation (40). While investigating the activation mechanism of NKCC1, Thastrup *et al* (41) revealed that NKCC1 could not be phosphorylated or activated during the deletion of SPAK/odd-skipped related transcription factor 1 (OSR1), and provided genetic evidence to confirm that SPAK/OSR1 serves an important role in controlling NKCC1 function. SPAK/NKCC1 regulates the coordinated transmembrane inflow and outflow of ions and water, which is necessary for the homeostasis of the volume of neurons, glial cells, endothelial cells and other cells, as well as for the integrity of the BBB (38). Furthermore, SPAK phosphorylation of NKCC1 has been associated with a number of neurological diseases, such as intracerebral hemorrhage (11) and schizophrenia (42). After ischemic stroke and other brain injuries, NKCC1 regulation of cell permeability changes the levels of extracellular fluid in inflammatory cells and blood extravasation, resulting in brain edema, inflammation and other secondary brain injury (43,44).

A study examining cerebral ischemia suggested that the WNK3/SPAK/NKCC1 signaling pathway is one of the key contributors to the formation of brain edema (45); a finding which was consistent with the current results. The present study found that the expression levels of p-SPAK in astrocytes and albumin exudation were increased after SBI in rats, which indicated that the BBB was destroyed, leading to brain edema. This phenomenon may be due to the effect of the increase of p-NKCC1 on cell ion transport (40). Previous studies have shown that inhibition of NKCC1 phosphorylation has a protective effect on brain edema, the mechanism of which is by reducing astrocyte swelling and BBB destruction (46-48). p-NKCC1 regulates the entry of Na^+, K^+, Cl^- and water into cells, changes the cellular volume and cytoskeletal structure of damaged cells, and can induce damage to astrocytes (47,49). Astrocytes are one of the components of BBB, and their apoptosis will lead to the destruction of BBB (50). Thus, the present study evaluated whether BBB function was impaired in SBI model rats using indicators associated with brain edema. It was identified that after SBI, albumin levels significantly rose and brain water content significantly increased, indicating that the function of the BBB was impaired. Furthermore, closantel inhibited SPAK activity, thereby reducing brain edema in SBI model rats.

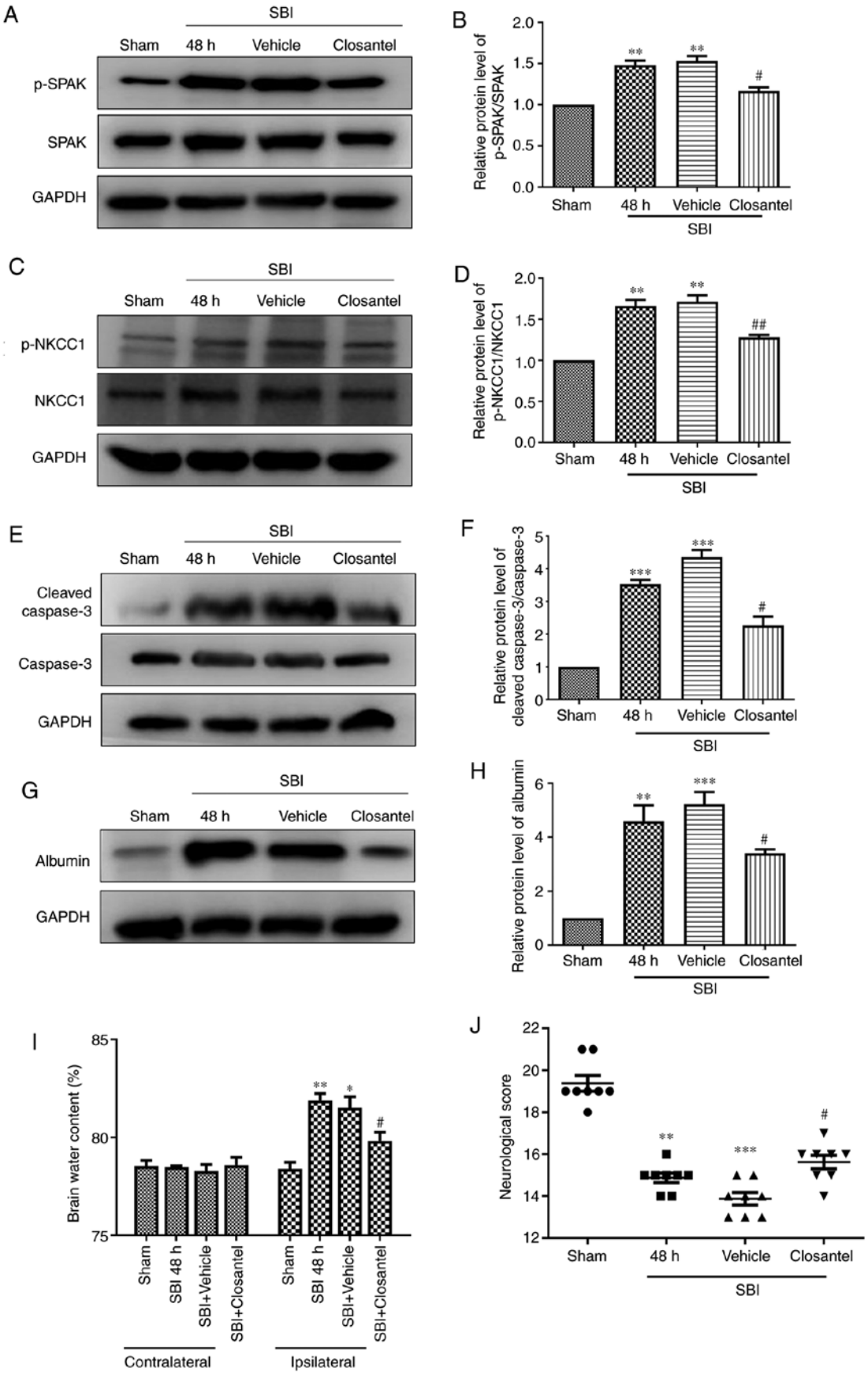

Figure 3. Protein expression levels of p-SPAK, p-NKCC1, albumin and cleaved-caspase-3 after the intervention of closantel at 48 h after SBI. Protein expression levels of (A and B) p-SPAK, (C and D) p-NKCC1, (E and F) cleaved-caspase-3 and (G and H) albumin were measured to evaluate the effect of closantel intervention on peripheral cortex injury at 48 h after SBI. (I) The brain water content of the bilateral hemispheres of the different groups was measured using the wet-dry method. (J) Neurological behavioral scores in SBI model rats after closantel intervention. Statistical analysis was performed using one-way ANOVA followed by Tukey's post hoc test. Data are presented as the mean ± SD (n=6 per group). *P<0.05, **P<0.01 and ***P<0.001 vs. sham; $^{\#}$P<0.05 and $^{\#\#}$P<0.01 vs. SBI + vehicle. SPAK, STE20/SPS1-related proline/alanine-rich kinase; NKCC1, Na^{+}-K^{+}-Cl^{-} cotransporter 1; SBI, surgical brain injury; p, phosphorylated.

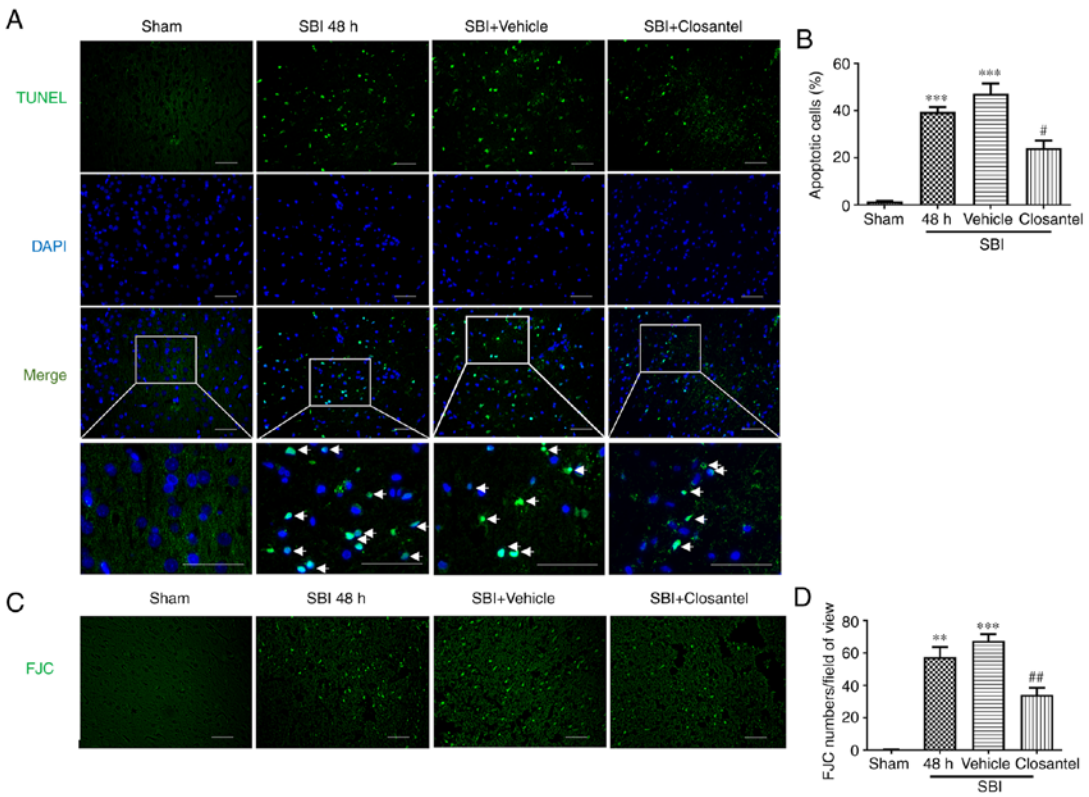

Figure 4. Effects of closantel intervention on peripheral cortical cell degradation and apoptosis at 48 h after SBI. Neuronal apoptosis was (A) determined by performing the TUNEL assay and (B) quantified. TUNEL (green) immunofluorescence labeled apoptotic cells and DAPI (blue) labeled nuclei. Neuronal degradation was (C) detected by performing FJC (green) staining and (D) quantified. Scale bar, 50 μm. The images for TUNEL, DAPI, FJC and Merge are at x200 magnification. Statistical analysis was performed using one-way ANOVA followed by Tukey's post hoc test. Data are presented as the mean ± SD (n=6 per group). **P<0.01 and ***P<0.001 vs. sham; $^{\#}$P<0.05 and $^{\#\#}$P<0.01 vs. SBI + vehicle. SBI, surgical brain injury; FJC, Fluoro-Jade C.

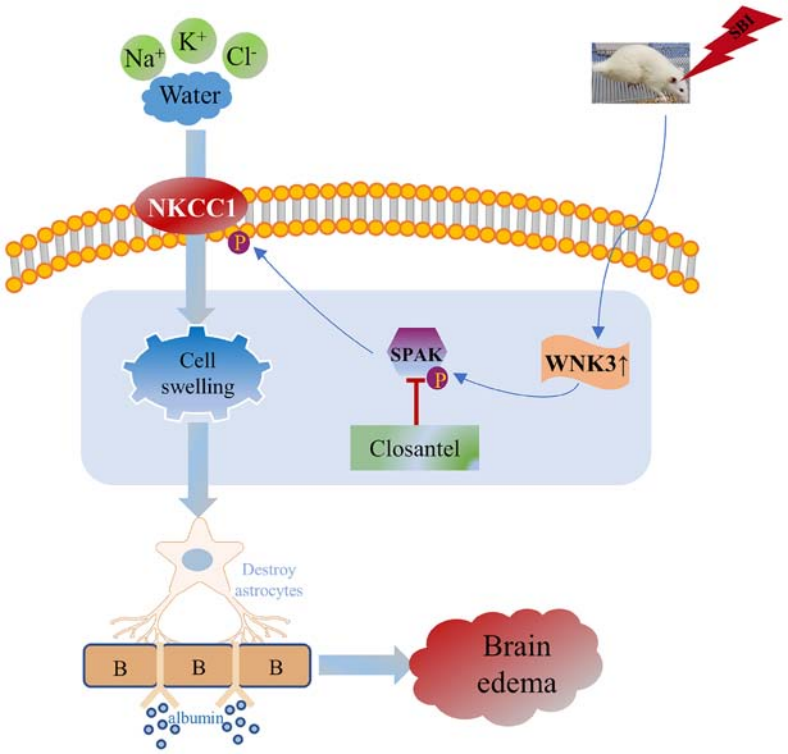

Figure 5. Schematic diagram illustrating the possible mechanisms underlying SPAK-mediated effects on SBI via regulating NKCC1. The present study indicated that SBI induced the rapid increase of p-SPAK expression, which lead to the increase of p-NKCC1. Subsequently, inorganic substances, such as Na^+, K^+, and Cl^-, flow into the astrocytes, causing the astrocytes to swell, damaging the stability of the BBB and eventually resulting in the brain edema. SPAK, STE20/SPS1-related proline/alanine-rich kinase; NKCC1, Na^+-K^+-Cl^- cotransporter 1; SBI, surgical brain injury; p, phosphorylated; WNK, WNK lysine deficient protein kinase 3; BBB, blood brain barrier.

Previous studies have reported that there was a significant correlation between brain edema and some neurological dysfunction after SBI injury in rats (51,52). The present results suggested that, compared with those in the sham group, neurobehavioral scores were significantly reduced in rats after SBI, which may be due to the degeneration and apoptosis of a large number of nerve cells after SBI, as well as the aggravation of brain edema, leading to neurological dysfunction. In a previous study of ischemic injury, SPAK knockout mice showed a 50% reduction in infarct size and cerebral edema, as well as significantly improved neurological function (8). The same result was observed when SPAK activity was inhibited in the current study. The present study revealed that after inhibiting p-SPAK using closantel, the expression level of p-NKCC1 was also decreased in SBI model rats. Compared with the SBI + vehicle group, albumin release was significantly decreased in SBI model rats treated with closantel. In addition, the apoptosis index was significantly decreased, the brain water content of the injured side was significantly decreased and the neurological function score was significantly increased in SBI model rats treated with closantel. These results suggested that inhibiting p-SPAK may mitigate SBI-induced secondary cerebral edema and reduce neuronal apoptosis, as well as ameliorate neurological dysfunction.

The mechanism of SBI causing secondary brain injury is highly complex. In the present study, p-SPAK was greatly increased after SBI, and the phosphorylation of the downstream p-NKCC1 signal was increased accordingly. A large number of ions and water enter nerve cells, which increases the cell volume and disrupts the cell structure, causing degeneration and apoptosis, destruction of the BBB, brain edema and neurological dysfunction, as demonstrated in the current study (Fig. 5). In the present study, it was identified that inhibition of the SPAK/NKCC1 signaling pathway alleviated secondary brain injury of SBI.

The current study has several limitations that should be discussed. The sample size of the study was small and only male rats were used. Therefore, it was not possible to investigate sex-mediated differences in the expression levels of p-SPAK and p-NKCC1 after SBI. Thus, this should be considered when interpreting the present results. In addition, it was not examined whether inhibition of p-NKCC1 would lead to changes in p-SPAK, which would further corroborate the current results. Moreover, the present study did not investigate whether p-SPAK agonists would lead to the upregulation of p-NKCC1 and further aggravate brain injury. Therefore, future studies are required to investigate further.

In conclusion, the present study showed that after SBI in rats, SPAK was activated, which could phosphorylate downstream NKCC1, and promote ions and water to enter cells, thus leading to cell apoptosis, which aggravated secondary brain injury. Inhibiting the activity of SPAK induced protective effects on the brain. These results indicated that SPAK may be potentially used as a prevention and control target for SBI.

Acknowledgements

Not applicable.

Funding

This work was supported by the Zhangjiagang Science and Technology Project (grant no. ZKS1914) and the Zhangjiagang Health Youth Science and Technology Project (grant no. ZJGQNKJ202030).

Availability of data and materials

The datasets used and/or analyzed during the current study are available from the corresponding author on reasonable request.

Authors' contributions

GC and BQD conceived and designed this study. YG and MW drafted and revised the manuscript. HG, MW and YG conducted the experiments. RG was responsible for analyzing and interpreting the data. FG and MS performed figure processing and data analysis. BQD and RG agreed to be responsible for all aspects of the work. BQD and RG confirm the authenticity of all the raw data. All authors have read and approved the final manuscript.

Ethics approval and consent to participate

All experiments received approval from the Institute of Animal Care Committee of Zhangjiagang Traditional Chinese Medicine Hospital (approval no. 2020-10-1; Suzhou, China).

Patient consent for publication

Not applicable.

Competing interests

The authors declare that they have no competing interests.

References

1. Zakhary G, Sherchan P, Li Q, Tang J and Zhang JH: Modification of kynurenine pathway via inhibition of kynurenine hydroxylase attenuates surgical brain injury complications in a male rat model. J Neurosci Res 98: 155-167, 2020.
2. Matchett G, Hahn J, Obenaus A and Zhang J: Surgically induced brain injury in rats: The effect of erythropoietin. J Neurosci Methods 158: 234-241, 2006.
3. Benggon M, Chen H, Applegate RL II and Zhang J: Thrombin preconditioning in surgical brain injury in rats. Acta Neurochir Suppl 121: 299-304, 2016.
4. Eser Ocak P, Ocak U, Sherchan P, Gamdzyk M, Tang J and Zhang JH: Overexpression of Mfsd2a attenuates blood brain barrier dysfunction via Cav-1/Keap-1/Nrf-2/HO-1 pathway in a rat model of surgical brain injury. Exp Neurol 326: 113203, 2020.
5. Chen JH, Hsu WC, Huang KF and Hung CH: Neuroprotective effects of collagen-glycosaminoglycan matrix implantation following surgical brain injury. Mediators Inflamm 2019: 6848943, 2019.
6. Kim CH, McBride DW, Sherchan P, Person CE, Gren ECK, Kelln W, Lekic T, Hayes WK, Tang J and Zhang JH: Crotalus helleri venom preconditioning reduces postoperative cerebral edema and improves neurological outcomes after surgical brain injury. Neurobiol Dis 107: 66-72, 2017.
7. Wu MY, Gao F, Yang XM, Qin X, Chen GZ, Li D, Dang BQ and Chen G: Matrix metalloproteinase-9 regulates the blood brain barrier via the hedgehog pathway in a rat model of traumatic brain injury. Brain Res 1727: 146553, 2020.

8. Zhao H, Nepomuceno R, Gao X, Foley LM, Wang S, Begum G, Zhu W, Pigott VM, Falgoust LM, Kahle KT, *et al*: Deletion of the WNK3-SPAK kinase complex in mice improves radiographic and clinical outcomes in malignant cerebral edema after ischemic stroke. J Cereb Blood Flow Metab 37: 550-563, 2017.
9. Gong YT, Wu MY, Tang JF, Shen JC, Li J, Gao R, Dang BQ and Chen G: Advances in the study of the role and molecular mechanism of withnolysine kinase 3 in nervous system diseases (Review). Mol Med Rep 23: 393, 2021.
10. Klug NR, Chechneva OV, Hung BY and O'Donnell ME: High glucose-induced effects on Na^+-K^+-$2Cl^-$ cotransport and Na^+/H^+ exchange of blood-brain barrier endothelial cells: Involvement of SGK1, PKCβII, and SPAK/OSR1. Am J Physiol Cell Physiol 320: C619-C634, 2021.
11. Wu D, Lai N, Deng R, Liang T, Pan P, Yuan G, Li X, Li H, Shen H, Wang Z and Chen G: Activated WNK3 induced by intracerebral hemorrhage deteriorates brain injury maybe via WNK3/SPAK/NKCC1 pathway. Exp Neurol 332: 113386, 2020.
12. Delpire E and Austin TM: Kinase regulation of Na^+-K^+-$2Cl^-$ cotransport in primary afferent neurons. J Physiol 588: 3365-3373, 2010.
13. Zhang J, Gao G, Begum G, Wang J, Khanna AR, Shmukler BE, Daubner GM, de Los Heros P, Davies P, Varghese J, *et al*: Functional kinomics establishes a critical node of volume-sensitive cation-Cl^- cotransporter regulation in the mammalian brain. Sci Rep 6: 35986, 2016.
14. Lykke K, Assentoft M, Hørlyck S, Helms HC, Stoica A, Toft-Bertelsen TL, Tritsaris K, Vilhardt F, Brodin B and MacAulay N: Evaluating the involvement of cerebral microvascular endothelial Na^+/K^+-ATPase and Na^+-K^+-$2Cl^-$ co-transporter in electrolyte fluxes in an in vitro blood-brain barrier model of dehydration. J Cereb Blood Flow Metab 39: 497-512, 2019.
15. Watanabe M and Fukuda A: Development and regulation of chloride homeostasis in the central nervous system. Front Cell Neurosci 9: 371, 2015.
16. Haas BR, Cuddapah VA, Watkins S, Rohn KJ, Dy TE and Sontheimer H: With-No-Lysine Kinase 3 (WNK3) stimulates glioma invasion by regulating cell volume. Am J Physiol Cell Physiol 301: C1150-C1160, 2011.
17. Zhang J, Karimy JK, Delpire E and Kahle KT: Pharmacological targeting of SPAK kinase in disorders of impaired epithelial transport. Expert Opin Ther Targets 21: 795-804, 2017.
18. Gagnon KB and Delpire E: Multiple pathways for protein phosphatase 1 (PP1) regulation of Na-K-2Cl cotransporter (NKCC1) function: The N-terminal tail of the Na-K-2Cl cotransporter serves as a regulatory scaffold for Ste20-related proline/alanine-rich kinase (SPAK) AND PP1. J Biol Chem 285: 14115-14121, 2010.
19. Cao-Pham AH, Urano D, Ross-Elliott TJ and Jones AM: Nudge-nudge, WNK-WNK (kinases), say no more? New Phytol 220: 35-48, 2018.
20. Alessi DR, Zhang J, Khanna A, Hochdörfer T, Shang Y and Kahle KT: The WNK-SPAK/OSR1 pathway: Master regulator of cation-chloride cotransporters. Sci Signal 7: re3, 2014.
21. Begum G, Yuan H, Kahle KT, Li L, Wang S, Shi Y, Shmukler BE, Yang SS, Lin SH, Alper SL and Sun D: Inhibition of WNK3 kinase signaling reduces brain damage and accelerates neurological recovery after stroke. Stroke 46: 1956-1965, 2015.
22. Zhang M, Cui Z, Cui H, Cao Y, Zhong C and Wang Y: Astaxanthin alleviates cerebral edema by modulating NKCC1 and AQP4 expression after traumatic brain injury in mice. BMC Neurosci 17: 60, 2016.
23. Tian Y, Guo SX, Li JR, Du HG, Wang CH, Zhang JM and Wu Q: Topiramate attenuates early brain injury following subarachnoid haemorrhage in rats via duplex protection against inflammation and neuronal cell death. Brain Res 1622: 174-185, 2015.
24. AlAmri MA, Kadri H, Alderwick LJ, Simpkins NS and Mehellou Y: Rafoxanide and closantel inhibit SPAK and OSR1 kinases by binding to a highly conserved allosteric site on Their C-terminal domains. ChemMedChem 12: 639-645, 2017.
25. Lin GM, Liu PY, Wu CF, Wang WB and Han CL: Perspective of future drugs targeting sterile 20/SPS1-related proline/alanine-rich kinase for blood pressure control. World J Cardiol 7: 306-310, 2015.
26. Kikuchi E, Mori T, Zeniya M, Isobe K, Ishigami-Yuasa M, Fujii S, Kagechika H, Ishihara T, Mizushima T, Sasaki S, *et al*: Discovery of Novel SPAK inhibitors that block WNK kinase signaling to cation chloride transporters. J Am Soc Nephrol 26: 1525-1536, 2015.
27. Wu BJ QC, Kong Q, Tan DM and Tan Y: Laboratory animal-Guideline for using animals in the education: Chinese Association for Laboratory Animal Sciences, 2017.
28. Akyol O, Sherchan P, Yilmaz G, Reis C, Ho WM, Wang Y, Huang L, Solaroglu I and Zhang JH: Neurotrophin-3 provides neuroprotection via TrkC receptor dependent pErk5 activation in a rat surgical brain injury model. Exp Neurol 307: 82-89, 2018.
29. Feng D, Wang B, Wang L, Abraham N, Tao K, Huang L, Shi W, Dong Y and Qu Y: Pre-ischemia melatonin treatment alleviated acute neuronal injury after ischemic stroke by inhibiting endoplasmic reticulum stress-dependent autophagy via PERK and IRE1 signalings. J Pineal Res: 62, 2017 doi: 10.1111/jpi.12395.
30. Zhang J, Xu X, Zhou D, Li H, You W, Wang Z and Chen G: Possible role of Raf-1 kinase in the development of cerebral vasospasm and early brain injury after experimental subarachnoid hemorrhage in rats. Mol Neurobiol 52: 1527-1539, 2015.
31. Zhao Y, Huang G, Chen S, Gou Y, Dong Z and Zhang X: Homocysteine aggravates cortical neural cell injury through neuronal autophagy overactivation following rat cerebral ischemia-reperfusion. Int J Mol Sci 17: 1196, 2016.
32. Wang YC, Cui Y, Cui JZ, Sun LQ, Cui CM, Zhang HA, Zhu HX, Li R, Tian YX and Gao JL: Neuroprotective effects of brilliant blue G on the brain following traumatic brain injury in rats. Mol Med Rep 12: 2149-2154, 2015.
33. Eroğlu H, Kaş HS, Oner L, Türkoğlu OF, Akalan N, Sargon MF and Ozer N: The in-vitro and in-vivo characterization of PLGA:L-PLA microspheres containing dexamethasone sodium phosphate. J Microencapsul 18: 603-612, 2001.
34. Ke K, Rui Y, Li L, Zheng H, Xu W, Tan X, Cao J, Wu X, Cui G and Cao M: Upregulation of EHD2 after intracerebral hemorrhage in adult rats. J Mol Neurosci 54: 171-180, 2014.
35. Bankstahl M, Breuer H, Leiter I, Märkel M, Bascuñana P, Michalski D, Bengel FM, Löscher W, Meier M, Bankstahl JP and Härtig W: Blood-brain barrier leakage during early epileptogenesis is associated with rapid remodeling of the neurovascular unit. eNeuro 5: ENEURO.0123-18.2018, 2018.
36. Yamazaki Y and Kanekiyo T: Blood-brain barrier dysfunction and the pathogenesis of Alzheimer's disease. Int J Mol Sci 18: 1965, 2017.
37. Lu KT, Cheng NC, Wu CY and Yang YL: NKCC1-mediated traumatic brain injury-induced brain edema and neuron death via Raf/MEK/MAPK cascade. Crit Care Med 36: 917-922, 2008.
38. Zhang J, Bhuiyan MIH, Zhang T, Karimy JK, Wu Z, Fiesler VM, Zhang J, Huang H, Hasan MN, Skrzypiec AE, *et al*: Modulation of brain cation-Cl^- cotransport via the SPAK kinase inhibitor ZT-1a. Nat Commun 11: 78, 2020.
39. Lee HA, Jeong H, Kim EY, Nam MY, Yoo YJ, Seo JT, Shin DM, Ohk SH and Lee SI: Bumetanide, the specific inhibitor of Na^+-K^+-$2Cl^-$ cotransport, inhibits 1alpha,25-dihydroxyvitamin D3-induced osteoclastogenesis in a mouse co-culture system. Exp Physiol 88: 569-574, 2003.
40. Huang H, Song S, Banerjee S, Jiang T, Zhang J, Kahle KT, Sun D and Zhang Z: The WNK-SPAK/OSR1 kinases and the cation-chloride cotransporters as therapeutic targets for neurological diseases. Aging Dis 10: 626-636, 2019.
41. Thastrup JO, Rafiqi FH, Vitari AC, Pozo-Guisado E, Deak M, Mehellou Y and Alessi DR: SPAK/OSR1 regulate NKCC1 and WNK activity: Analysis of WNK isoform interactions and activation by T-loop trans-autophosphorylation. Biochem J 441: 325-337, 2012.
42. Yang SS, Huang CL, Chen HE, Tung CS, Shih HP and Liu YP: Effects of SPAK knockout on sensorimotor gating, novelty exploration, and brain area-dependent expressions of NKCC1 and KCC2 in a mouse model of schizophrenia. Prog Neuropsychopharmacol Biol Psychiatry 61: 30-36, 2015.
43. Luo WD, Min JW, Huang WX, Wang X, Peng YY, Han S, Yin J, Liu WH, He XH and Peng BW: Vitexin reduces epilepsy after hypoxic ischemia in the neonatal brain via inhibition of NKCC1. J Neuroinflammation 15: 186, 2018.
44. Simard JM, Kahle KT and Gerzanich V: Molecular mechanisms of microvascular failure in central nervous system injury-synergistic roles of NKCC1 and SUR1/TRPM4. J Neurosurg 113: 622-629, 2010.
45. LeVine SM: Albumin and multiple sclerosis. BMC Neurol 16: 47, 2016.
46. Lee YC, Kao ST and Cheng CY: Acorus tatarinowii Schott extract reduces cerebral edema caused by ischemia-reperfusion injury in rats: Involvement in regulation of astrocytic NKCC1/AQP4 and JNK/iNOS-mediated signaling. BMC Complement Med Ther 20: 374, 2020.

47. Taherian M, Norenberg MD, Panickar KS, Shamaladevi N, Ahmad A, Rahman P and Jayakumar AR: Additive effect of resveratrol on astrocyte swelling post-exposure to ammonia, ischemia and trauma in vitro. Neurochem Res 45: 1156-1167, 2020.
48. Zhang M, Cui Z, Cui H, Wang Y and Zhong C: Astaxanthin protects astrocytes against trauma-induced apoptosis through inhibition of NKCC1 expression via the NF-kappaB signaling pathway. BMC Neurosci 18: 42, 2017.
49. Luo L, Guan X, Begum G, Ding D, Gayden J, Hasan MN, Fiesler VM, Dodelson J, Kohanbash G, Hu B, *et al*: Blockade of cell volume regulatory protein NKCC1 increases TMZ-induced glioma apoptosis and reduces astrogliosis. Mol Cancer Ther 19: 1550-1561, 2020.
50. Campisi M, Shin Y, Osaki T, Hajal C, Chiono V and Kamm RD: 3D self-organized microvascular model of the human blood-brain barrier with endothelial cells, pericytes and astrocytes. Biomaterials 180: 117-129, 2018.
51. McBride DW, Wang Y, Adam L, Oudin G, Louis JS, Tang J and Zhang JH: Correlation between subacute sensorimotor deficits and brain edema in rats after surgical brain injury. Acta Neurochir Suppl 121: 317-321, 2016.
52. Gong Y, Wu M, Shen J, Tang J, Li J, Xu J, Dang B and Chen G: Inhibition of the NKCC1/NF-κB signaling pathway decreases inflammation and improves brain edema and nerve cell apoptosis in an SBI Rat model. Front Mol Neurosci 14: 641993, 2021.